PLOS ONE

RESEARCH ARTICLE

Effects of ursolic acid on sub-lesional muscle pathology in a contusion model of spinal cord injury

Gregory E. Bigford[1,2]*, Andrew J. Darr[3], Valerie C. Bracchi-Ricard[4], Han Gao[1,2], Mark S. Nash[1,2,5], John R. Bethea[4]

1 The Miami Project to Cure Paralysis, Miami, Florida, United States of America, **2** Department of Neurological Surgery, University of Miami Miller School of Medicine, Miami, Florida, United States of America, **3** Department of Health Sciences Education, University of Illinois College of Medicine at Peoria, Peoria, Illinois, United States of America, **4** Department of Biology, Drexel University, Philadelphia, Pennsylvania, United States of America, **5** Department of Rehabilitation Medicine, University of Miami Miller School of Medicine, Miami, Florida, United States of America

* gbigford@med.miami.edu

OPEN ACCESS

Citation: Bigford GE, Darr AJ, Bracchi-Ricard VC, Gao H, Nash MS, Bethea JR (2018) Effects of ursolic acid on sub-lesional muscle pathology in a contusion model of spinal cord injury. PLoS ONE 13(8): e0203042. https://doi.org/10.1371/journal.pone.0203042

Editor: Andrew Philp, Garvan Institute of Medical Research, AUSTRALIA

Received: March 22, 2018

Accepted: August 14, 2018

Published: August 29, 2018

Data Availability Statement: All relevant data are within the paper and its Supporting Information files.

Funding: This work was supported by the Miami Project to Cure Paralysis. The funders had no role in study design, data collection and analysis, decision to publish, or preparation of the manuscript.

Competing interests: The funders had no role in study design, data collection and analysis, decision to publish, or preparation of the manuscript.

Abstract

Spinal Cord Injury (SCI) results in severe sub-lesional muscle atrophy and fiber type transformation from slow oxidative to fast glycolytic, both contributing to functional deficits and maladaptive metabolic profiles. Therapeutic countermeasures have had limited success and muscle-related pathology remains a clinical priority. mTOR signaling is known to play a critical role in skeletal muscle growth and metabolism, and signal integration of anabolic and catabolic pathways. Recent studies show that the natural compound ursolic acid (UA) enhances mTOR signaling intermediates, independently inhibiting atrophy and inducing hypertrophy. Here, we examine the effects of UA treatment on sub-lesional muscle mTOR signaling, catabolic genes, and functional deficits following severe SCI in mice. We observe that UA treatment significantly attenuates SCI induced decreases in activated forms of mTOR, and signaling intermediates PI3K, AKT, and S6K, and the upregulation of catabolic genes including FOXO1, MAFbx, MURF-1, and PSMD11. In addition, UA treatment improves SCI induced deficits in body and sub-lesional muscle mass, as well as functional outcomes related to muscle function, motor coordination, and strength. These findings provide evidence that UA treatment may be a potential therapeutic strategy to improve muscle-specific pathological consequences of SCI.

Introduction

Traumatic spinal cord injury (SCI) incites numerous pathophysiological changes and persistent metabolic abnormalities [1–5] that contribute to long-term effects on body systems. [6, 7] Physical limitations related to movement, musculoskeletal activity and weight-bearing contribute to deleterious changes in body composition, typified by rapid and long-term declines in metabolically active muscle-mass [8–16] and bone [17–23], as well as stark increases in central

adiposity [24–27] which contributes to the maladaptive metabolic profile in SCI. As a result, there is a prevalence of co-morbid risk factors for *cardiometabolic* disorders in chronic SCI including obesity [28], dyslipidemia [24–26, 29–37], glucose intolerance, and insulin resistance [5, 36], symptoms that are indicative of cardiovascular disease (CVD) and diabetes. Notably, CVD has emerged as the leading cause of mortality in chronic SCI. [38, 39]

Sub-lesional skeletal muscles undergo severe pathological consequences following human SCI. Muscle mass is diminished by as much as 48% as early as 6-weeks post-SCI [13], and atrophy ranges from 30–60% depending on muscle type, duration and completeness of injury. [22] These changes coincide with muscle fiber-type transformation from slow oxidative Type I to fast glycolytic Type II [8, 12, 40–44], diminishing skeletal muscle oxidative phenotype that is linked to insulin resistance and progression of metabolic syndrome.

In SCI, a reduction in anabolic hormones such as testosterone, insulin and insulin-like growth factor-1 (IGF-1) [45, 46] may contribute to reduced IGF-1 receptor activation of metabolically-linked signaling pathways in muscle. It is well-established that activation of phosphoinositide-3 kinase (PI3K)/Akt and downstream anabolic target mammalian target of rapamycin (mTOR) regulate, in part, skeletal muscle protein synthesis, cell growth and metabolism. [47–49] Additionally, mTOR-activation regulates the transcription factor fork-head box protein 01 (FOXO1), which is associated with catabolic genes involved with ubiquitin-proteasomal degradation in muscle. [50] mTOR is a complex signal integrator that regulates both anabolic and catabolic processes in the muscle, however these processes are not well defined in SCI.

Recently, interest in the naturally occurring lipophilic pentacyclic triterpenoid ursolic acid (UA) in medical research has grown significantly due to its pharmacological effects and low toxicity. [51] For example, studies have shown that UA enhances insulin- and IGF-mediated phosphorylation of AKT, S6K1 and FOXO1 in skeletal muscle. [52, 53] Importantly, it was reported that UA inhibits skeletal muscle atrophy associated with denervation and induces skeletal muscle hypertrophy in the absence of an atrophy stimulus [53], in addition to its documented ability to augment muscle strength [54] and stimulate mTORC1 signaling in skeletal muscle. [55] Although implicated in skeletal muscle metabolic and growth signaling, the effects of UA on muscle pathophysiology has not been explored in SCI. In this study, we investigated UA as an anabolic stimulator of metabolically-linked signaling pathways in muscle and explored phenotypic outcomes in sub-lesional muscle following traumatic SCI. Our primary objectives are to examine following experimental SCI i. intracellular mTOR signaling, ii. the expression of related catabolic genes, and iii. the effects on these outcomes with UA treatment. We hypothesize that SCI will i. reduce growth pathways via mTOR signaling, ii. increase the expression of catabolic genes, and iii. UA will attenuate these SCI-induced changes. In addition, we aim to examine the effect of SCI on physical and functional measures, and whether UA-induced improvement in muscle signaling translates to improvements in these outcome measures.

Materials and methods

All animal protocols were approved by the University of Miami Institutional Animal Care and Use Committee (IACUC) and are in accordance with National Research Council guidelines for the care and use of laboratory animals. Animals were group (socially) housed in a temperature- and humidity- controlled rodent vivarium, maintained on a reverse 12-hour light/dark cycle, and given food and water *ad libitum*. No additional environmental enrichment was provided due to its reported effects on the nervous system, including neurogenesis and levels of inflammation, which may affect experimental outcomes. Animals were acclimated for seven

days prior to study experiments, which included being handled daily to get used to human contact and minimize distress. To ensure minimal suffering prior to any surgical procedure, to demonstrate that the animal was completely under anesthesia, we examined hind limb reflex by pulling and straightening the hind limb to determine when the limb is flaccid. Secondly, we pinched the hind paw for the lack of pain response. The flaccidity of the limb and the absence of reflex automatic movements at the pinching of the tail indicated a deep state of anesthesia. Following surgical procedures, animals were administered buprenorphine (0.1 mg/kg) BID for 3-days post surgery and PRN thereafter. Animals were examined twice daily for post-stress health status by observation of activity level, respiratory rate, and general physical condition. Body weight was monitored every other day. Excessive weight loss (>20%) and decreased grooming behavior was considered as criteria for early exclusion from the study and/or euthanasia. Physical conditions such as moribund state, dehydration, and anorexia were also considered as criteria for early termination. Euthanasia was carried out by carbon dioxide inhalation according to the recommendations for euthanasia detailed in the 2007 Report of the American Veterinary Medical Association's (AVMA) Panel on Euthanasia. Euthanasia was performed in a manner to avoid animal distress. The chamber was not pre-filled with gas before placing the animals inside, and the rate of CO2 flow into the chamber was slowly increased. Animals were in a deep state of sleep after one minute, then the CO2 flow rate was increased for another four minutes. After CO2 exposure, confirmation of termination was accomplished by cervical dislocation.

Traumatic SCI and UA administration

Surgeries were performed at the Animal and Surgical Core Facility of the Miami Project to Cure Paralysis according to protocols approved by the IACUC of the University of Miami. Contusion injury was induced with the Infinite Horizon Impactor device adapted to the mouse. The infinite Horizon impactor device has been established in producing precise, graded contusion, with reproducible lesion volume and functional outcomes assessed using Basso, Beattie, Bresnahan (BBB) and Basso Mouse Scale (BMS) [56] open-field locomotor rating scales. [57] In brief, Adult female C57Bl/6 mice (12-weeks old, ~20g; Jackson Laboratories) were anesthetized with an intraperitoneal injection of ketamine (80–100 mg/kg) and xylazine (10 mg/kg). Complete anesthetization was determined by the lack of a stereotypical retraction of the hind-paw in response to a nociceptive stimulus. Mice were then subjected to a laminectomy at vertebrae T9 and the exposed spinal cord was injured at a predetermined impact force of 70 kdynes (severe injury). Sham-operated animals underwent all surgical procedures, including laminectomy, but their spinal cords were not injured. After surgery, animals were housed separately and treated with subcutaneous lactated Ringer's solution to prevent dehydration. Manual bladder expression was performed twice daily. Prophylactic antibiotic gentamicin was administered daily for 7 days to prevent urinary tract infections. SCI animals were randomized to 3 groups: SCI, SCI/UA (TCI America) [200 mg/Kg UA dissolved in corn oil (CO) (Spectrum Chemical Mftg Corp); i.p.], and SCI/Vehicle (CO only). UA was administered using a previously reported [53] dose that resulted in positive and effective changes in mTOR signaling and catabolic gene expression. UA/CO treatments were administered once daily until time of sacrifice. Animal tissue was harvested 1-, 2-, or 4-weeks post SCI, snap-frozen in liquid nitrogen and stored at –80˚C until the time of assay.

Protein extraction and immunoblot analysis

Mice soleus muscle tissues were harvested and homogenized in a Dounce homogenizer with extraction/lysis buffer (20 mM Tris–HCl, pH: 7.5, 150 mM NaCl, 1% Triton X-100; 1 mM ethylenediaminetetraacetic acid, 1 mM ethylene glycol tetraacetic acid, 2.5 mM pyrophosphate, 1

mM β-glycerophosphate) containing protease and phosphatase inhibitor cocktails and then centrifuged at 15 000 x g for 2 minutes. Lysates were mixed with 2x Laemmli loading buffer. Equal amounts of protein were resolved on 10–20% gradient Tris-HCl pre-casted gels, to separate proteins with a wide range of molecular weights, transferred to polyvinylidene fluoride (PVDF) membranes and placed in blocking buffer (0.1% Tween-20, 0.4% I-block in PBS) overnight. Membranes were then incubated with primary antibodies followed by the appropriate HRP-conjugated secondary antibody (1:1000). Visualization of the signal was obtained with an enhanced chemiluminescence substrate using a Phototope- HRP detection kit (Cell Signaling Technology®). Quantification of bands corresponding to phosphor-PI3K, phosphor-AKT, phosphor-mTOR and phosphor-S6K was made using the ChemiDoc Touch™ Imaging System (BioRad), and normalized to β-Actin, $PI3K^{Total}$, AKT^{Total}, $mTOR^{Total}$, or $S6K^{Total}$, where appropriate.

Total ribonucleic acid (RNA) isolation and quantitative RT-PCR

Total RNA was isolated from mouse soleus using TRIZOL Reagent (Invitrogen) according to manufacturer's instructions. 5 ug of RNA were reverse transcribed using SuperScript III First Strand Synthesis System for RT-PCR (Invitrogen). Real-time PCR was performed with the Applied Biosystems 7300 Real-time PCR System on samples amplified with Rotor-Gene SYBR Green PCR Kit (Qiagen) and primers for the transcription factor FoxO1, the muscle-restricted E3 ligases Atrogin-1/MAFbx, MURF-1, and the proteasomal assembly protein 26S proteasome non-ATPase regulatory subunit 11 (PSMD11) (Table 1). Relative expression (as fold change) of target genes were calculated after normalization to Beta-Actin using the $2^{-\Delta\Delta Ct}$ method.

Body and soleus muscle mass

Body mass discriminated to 0.1g was measured on a calibrated analytic balance (Data Weighing Systems) at baseline (before survival surgery); and daily thereafter until necropsy (1-, 2-, or 4-weeks post-surgery). Soleus muscle tissue was harvested at necropsy as described above. Tissue wet weight was measured on a calibrated microbalance (Data Weighing Systems) to 0.01 mg, before being snap frozen using liquid nitrogen and stored at -80˚C until the time of assay.

Behavioral and motor function analysis

Open field and BMS test. The open field test was performed on experimental mice in an odor-free, non-transparent square arena as previously described. The arena was divided into three zones (wall, inter and center) and mouse behavior was recorded over a 5 min period using a high resolution, video camera. Total number of lines crossed, time spent in each zone and stereotypical behaviors such as grooming and rearing were analyzed and expressed as number of events. Mice that did not enter all three zones or cross a minimum of 50 lines

Table 1. Gene primers for quantitative RT-PCR.

Gene	Genebank #	Primer Pairs	Tm/Product
FOXO1	NM_019739	Forward: 5′—CTACGAGTGGATGGTGAAGAGC Reverse: 5′—CCAGTTCCTTCATTCTGCACTC	64.9/5552
MAFbx	NM_026346	Forward: 5'—CTTCTCGACTGCCATCCTGGAT Reverse: 5'—TCTTTTGGGCGATGCCACTCAG	68.7/6936
Murf-1	NM_001039048	Forward: 5'—TACCAAGCCTGTGGTCATCCTG Reverse: 5'—ACGGAAACGACCTCCAGACATG	68.2/1886
PSMD11	XM_011249223	Forward: 5'—CAGCAGAGGAGAAGGACTGGAA	67/2693

https://doi.org/10.1371/journal.pone.0203042.t001

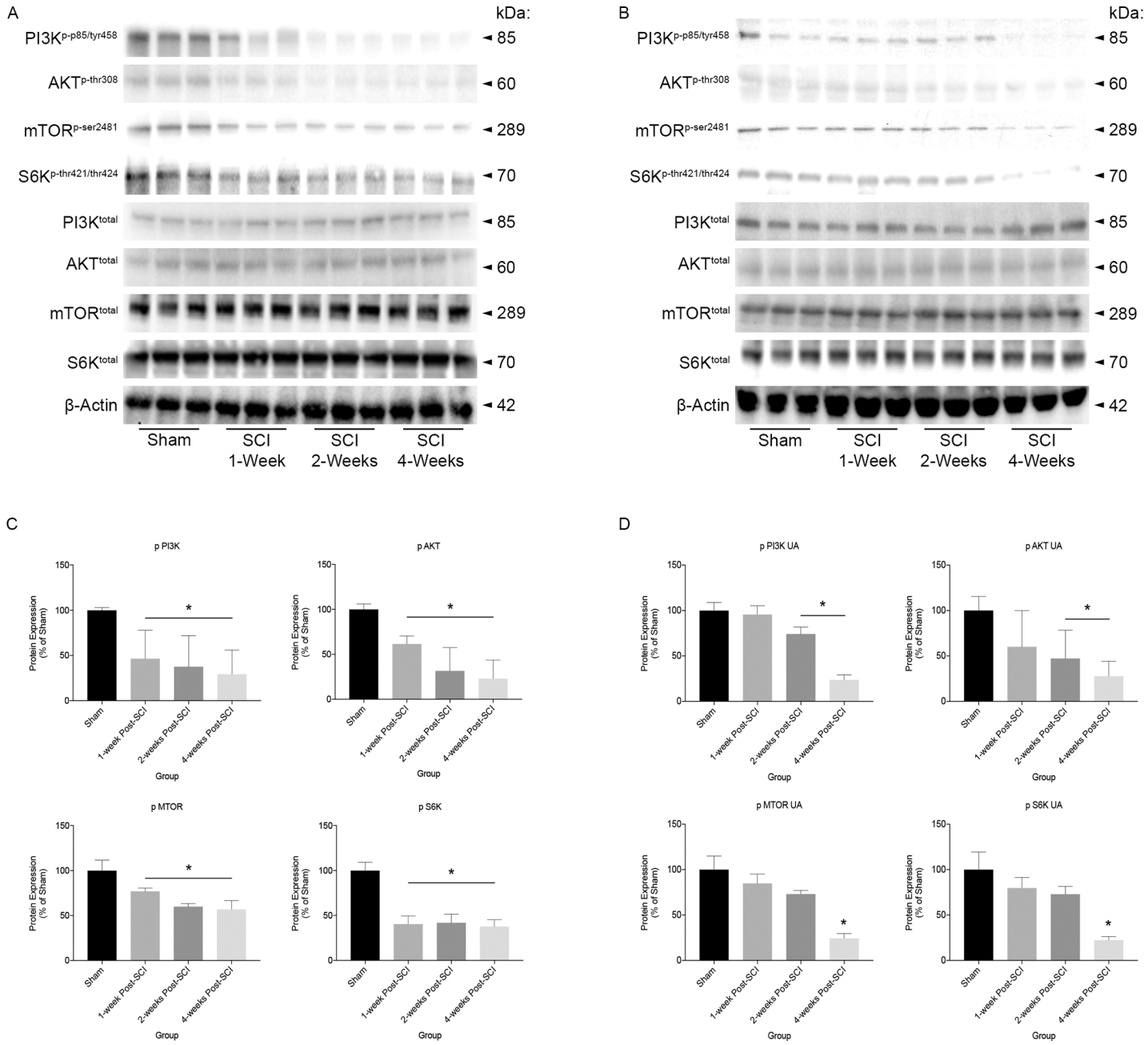

Fig 1. Phosphorylated protein expression of PI3K, AKT, mTOR, and S6K in soleus muscle from sham, SCI, and SCI-UA treated mice. At 1-, 2- and 4-weeks post-SCI, phosphorylated forms of PI3K, AKT, mTOR, and S6K were significantly decreased when compared to sham controls (**A,C**). In UA treated mice, there was no longer a significant difference at 1-week post-SCI compared to sham controls for all signaling intermediates. At 2- and 4-weeks post-SCI, there was a significant decrease in phosphorylated PI3K and AKT, and by 4-weeks only was there a significant decrease in phosphorylated mTOR and S6K compared to sham controls (**B,D**). $^{*}p < 0.05$.

https://doi.org/10.1371/journal.pone.0203042.g001

during the 5 min trial were excluded. Scoring of locomotor hind-limb performance in the open field was performed with the BMS, [56] a 0 to 9 rating system based on a modification of the BBB and specifically designed for the mouse. Under blind conditions, a team of two investigators evaluates the mice over a 5-min time period 1 day after SCI and bi-weekly thereafter.

Rotarod time trial test. Motor coordination and balance were tested on the accelerating rotarod cylinder (Rotamex 4/8, Columbus Instruments). The test consisted of 5-day pre-

training (days 1 to 5) followed by testing days at 2- and 4-weeks Post-SCI. The cylinder rotated at increasing speed and constant acceleration (from 10 to 60 rpm over 10 min period). The total time spent on the rod prior to fall was recorded and non-walking behaviors, such as passive clinging to the rod, were manually corrected. Each trial consisted of the average of 4 sessions. After each session, the mice were transferred back to their cage and allowed to rest for 20 min to avoid exhaustion and minimize stress. Mice that could not maintain their balance on the rod for a minimum of 60 seconds during pre-training were excluded from analysis.

Grip strength test. All experimental mice underwent analysis of hind-limb peak force (muscle strength) using the grip-strength test. Hind-limb grip strength was assessed using a digital force gauge (Chatillon DFIS2, Ametek) which generates a measure of neuromuscular function as maximal muscle strength—with the unit of force measured being delivered in Newton's. The test consisted of a baseline assessment prior to surgery, followed by testing days at 2- and 4-weeks Post-SCI. Force values were calculated average of 5-trials.

Statistical analysis

Between group differences were analyzed using one-way analysis of variance (ANOVA), followed by Tukey post hoc comparison and reflect fold change (immunoblot and mRNA analysis) and absolute change (soleus muscle mass and all behavioral analysis) from sham-control animals. For body mass, between group and within group differences across time were analyzed using a mixed-model analysis of variance (ANOVA), followed by Tukey post hoc comparison (GraphPad, Prism) and reflect fold change from sham control animals. Data are expressed as mean ± SEM. A significance level of $p \leq 0.05$ was accepted as different from control. n = 6 for each group, and each sample was run in triplicate (immunoblots) or duplicate (mRNA). n = 8–10 for each group (behavioral testing).

Results

UA treatment attenuates the loss of IGF-1/mTOR signaling observed following SCI

To define whether SCI alters activation of IGF-1/mTOR signaling cascades, and examine the effect of UA treatment, soleus muscle lysates from control (sham) and injured animals at various times after trauma were analyzed by immunoblotting procedures (Fig 1). We determined that SCI induced a significant decrease in the activated (phosphorylated) forms of PI3K, AKT, mTOR, and S6K at 1-, 2-, and 4-weeks post SCI (all P's, 0.01), when compared to sham control (Fig 1A and 1C). However, in mice treated with UA, changes in expression of activated forms of all proteins examined were no longer significant at 1-week post-SCI compared to sham. By 2- and 4-weeks post-SCI phosphorylated PI3K (P's < 0.01) and AKT (P's < 0.05) were again significantly diminished, and only at 4-weeks post-SCI were phosphorylated mTOR and S6K significantly less compared to sham (both P's < 0.01) (Fig 1B and 1D). Thus, SCI induces a significant decrease in activated mTOR and upstream signaling intermediates, and treatment with UA attenuates these signaling deficits acutely, delaying the effects of SCI on this IGF-1/mTOR pathway.

UA treatment reduces FOXO1, MAFbx, MURF-1, and PSMD11 gene upregulation that occurs acutely following SCI

To investigate activation of catabolic processes in soleus muscle extracts from our experimental groups, we examined the gene expression levels of the transcription factor FOXO1, the muscle-restricted E3 ligases Atroginin/MAFbx and muscle ring finger-1 (MuRF-1), and the

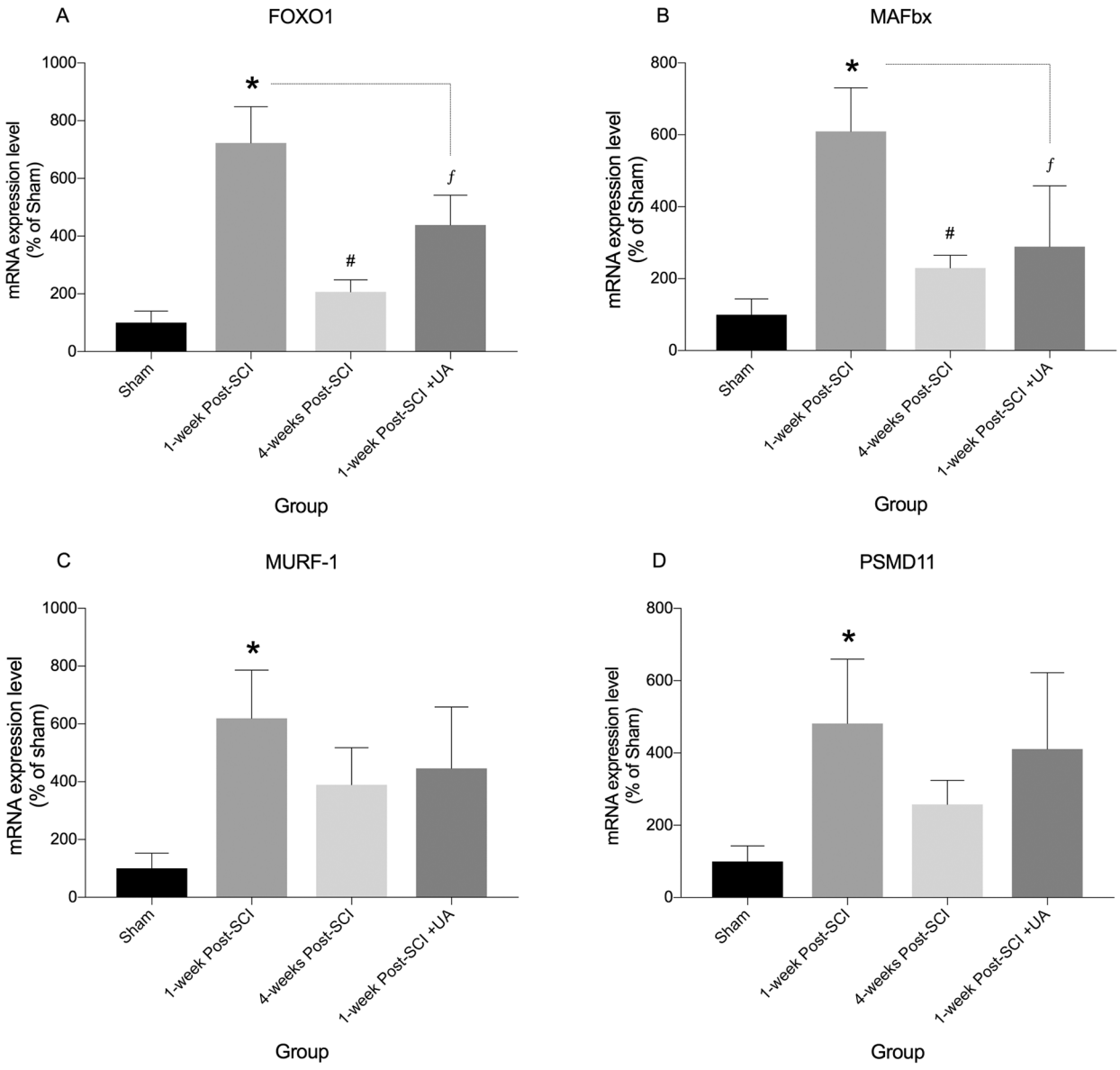

Fig 2. mRNA analysis of FOXO1, MAFbx, MURF-1, and PSMD11 in soleus muscle from Sham, SCI, and SCI-UA treated mice. mRNA expression of FOXO1, MAFbx, MURF-1 and PSMD11 were significantly greater at 1-week post-SCI (*) compared to sham control (**A-D**). By 4-weeks post-SCI, FOXO1 and MAFbx mRNA were significantly reduced compared to 1-week (**A,B** #) post-SCI and no longer significantly different from sham controls. At 4-weeks post-SCI Murf-1 and PSMD11 mRNA were observably but not significantly lower than 1-week post-SCI and no longer statistically different from sham controls (**C,D**). In UA treated mice, mRNA expression of FOXO1 and MAFbx were significantly less compared to untreated SCI mice at 1-week post-SCI (**A,B** *f*), and mRNA of MURF-1 and PSMD11 were observably but not statistically different at the same time-point compared to sham controls (**C,D**). $^{*,\#,f}p < 0.05$.

https://doi.org/10.1371/journal.pone.0203042.g002

proteasomal protein PSMD11, using quantitative rt-PCR (Fig 2). Significant increases in mRNA expression were observed in all genes examined when compared to sham control, and peaked at 1-week post-SCI (FOXO1, MAFbx, P's < 0.01; MuRF-1, PSMD11, P's < 0.05) (Fig 2A–2D). By 4-weeks post-SCI, levels of FOXO1 and MAFbx mRNA were lower than levels observed at 1-week post-SCI and were commensurate with those of sham controls (Fig 2A and 2B). By 4-weeks post-SCI, MURF-1 and PSMD11 mRNA levels were no longer significantly different from those of sham animals, however the lower levels observed relative to 1-week

post-SCI were not statistically significant (Fig 2C and 2D). Furthermore, in mice receiving UA treatment, at 1-week post-SCI, FOXO1 and MAFbx mRNA expression was significantly lower when compared to mice at 1-week post-SCI without treatment (i.e. peak expression; both P's < 0.05) (Fig 2A and 2B). Non-significant decreases in MURF-1 and PSMD11 were also observed (Fig 2C and 2D). These results provide evidence that several catabolic genes associated with proteolysis are upregulated in soleus muscle acutely following SCI, and UA treatment is capable of thwarting these early effects.

UA treatment preserves body and soleus muscle mass following SCI

Body mass was measured at baseline (just prior to injury) and daily for 4-weeks post-SCI. Acutely post-SCI, there was a rapid and stark decrease in body mass which remained significant from 1-day post-SCI through 28 days (all P's < 0.01 days 1–20; all P's < 0.05 days 21–28) when compared to sham-control (Fig 3A). There was a progressive recovery of body mass in

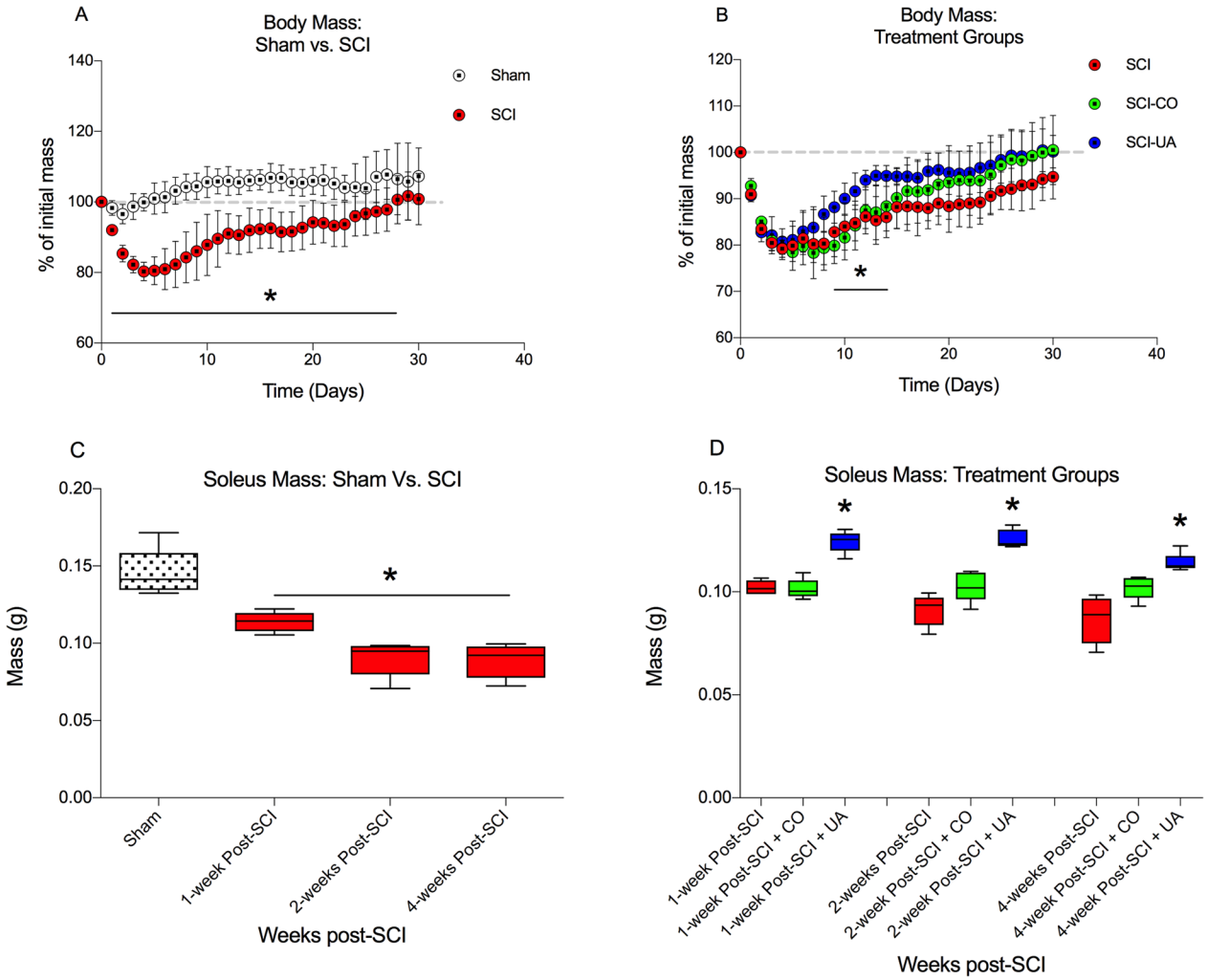

Fig 3. UA treatment preserves body and soleus muscle mass following SCI. A. Body mass was significantly reduced between 1–28 days post-SCI compared to sham controls, and progressively recovered to baseline by ~4-weeks post-SCI. **B.** UA treatment significantly increased body mass compared to SCI-CO (vehicle) and SCI alone between days 9–11 and 12–14, respectively. **C.** Soleus muscle mass was significantly reduced at 1-, 2-, and 4-weeks post-SCI compared to sham. **D.** UA treatment significantly increased Soleus muscle mass at all time-points compared to SCI-CO and SCI alone. $^{*}p < 0.05$.

https://doi.org/10.1371/journal.pone.0203042.g003

SCI mice which reached baseline level by ~4-weeks post-SCI, although still observably lower than sham by this time point. When compared to SCI and SCI-CO (vehicle control), in mice treated with UA (SCI-UA), there was an observable upward trend in body mass throughout the 4-week timeline, reaching significance at day 9–11 (all P's < 0.05) compared to SCI-CO and day 12–14 (all P's < 0.05) compared to SCI alone (Fig 3B). In addition, total soleus muscle mass (left and right) was significantly lower in tissue harvested at 1-, 2-, and 4-weeks post-SCI (all P's < 0.01), when compared to sham control (Fig 3C). In SCI-UA, soleus muscle mass was significantly greater than SCI and SCI-CO control at all time-points post-SCI (1- and 2-weeks post-SCI, P's <0.01; 4-weeks post-SCI, P's <0.05) (Fig 3D). These data demonstrate that UA treatment may aide body mass maintenance, and importantly, preserve sub-lesional muscle mass after SCI.

UA improves functional motor scores and measures of muscle coordination and sub-lesional muscle force production following SCI

To confirm the effects of SCI and UA treatment on sub-lesional motor function, we performed the BMS open field locomotor test, rotarod time trial, and hind-limb grip strength test (Fig 4). At 1-day post-SCI, significant deficits in BMS composite scores were observed in SCI, SCI-CO, and SCI-UA mice compared to sham controls (all P's < 0.01) (Fig 4A). By 2- and 4-weeks post-SCI, BMS scores across all experimental groups remained significantly lower than sham controls, however, there was an observable yet statistically non-significant increase in BMS sores in SCI-UA compared to SCI-CO and SCI animals alone. Additionally, at 2- and 4-weeks post-SCI, all experimental groups showed significant deficits in Rotarod time trials when compared to sham controls (all P's < 0.01) (Fig 4B). Moreover, SCI-UA mice were significantly greater compared to SCI-CO and SCI alone at the same time points post-SCI (both P's < 0.05). Similarly, grip strength at 2- and 4-weeks post-SCI were significantly diminished in all experimental groups compared to sham controls (2-weeks post-SCI, $P < 0.05$; 4-weeks post-SCI, $P <0.01$) (Fig 4C), and SCI-UA mice exhibited significantly greater grip strength compared to SCI-CO and SCI alone at the same time points post-SCI (both P's < 0.05). These results demonstrate that UA improves hind-limb function, motor coordination and grip strength after SCI.

Discussion

In this study, we show that the natural compound UA improves anabolic IGF-1/mTOR signaling cascades in soleus muscle after experimental SCI. We also show that SCI-induced upregulation of several proteolytic genes, are reduced following treatment with UA. In addition, these genetic and biochemical effects of UA improve physical measures including: body and soleus muscle mass, and measures of muscle function, motor coordination and strength. These findings suggest that UA is a potential therapeutic adjunctive for physical deconditioning and motor deficits observed after SCI.

It is well established that the principal consequences of SCI on sub-lesional muscle include muscle atrophy [13, 22] and a slow and progressive transformation of fiber type resulting in a predominance of the glycolytic (type II) isoform. [8, 12, 40–44] These changes in the muscle promote two major outcomes: functional deficits of the paralyzed muscle due to the neurological insult and the development of metabolic dysfunction and cardiometabolic syndrome (CMS) risk factors. With respect to functional decline, previous reports using tests of maximum voluntary contraction [58] and isometric force production [59–61] have characterized atrophic muscle as having low contractile force. [62] Moreover, this muscle weakness is associated with rapid muscle fatigability, in both humans [12, 40–42] and animal models [43] [Reviewed in [63]], due to the predominantly glycolytic phenotype. Importantly, these pathological adaptations of the muscle have limited the "functional" recovery intended with leading

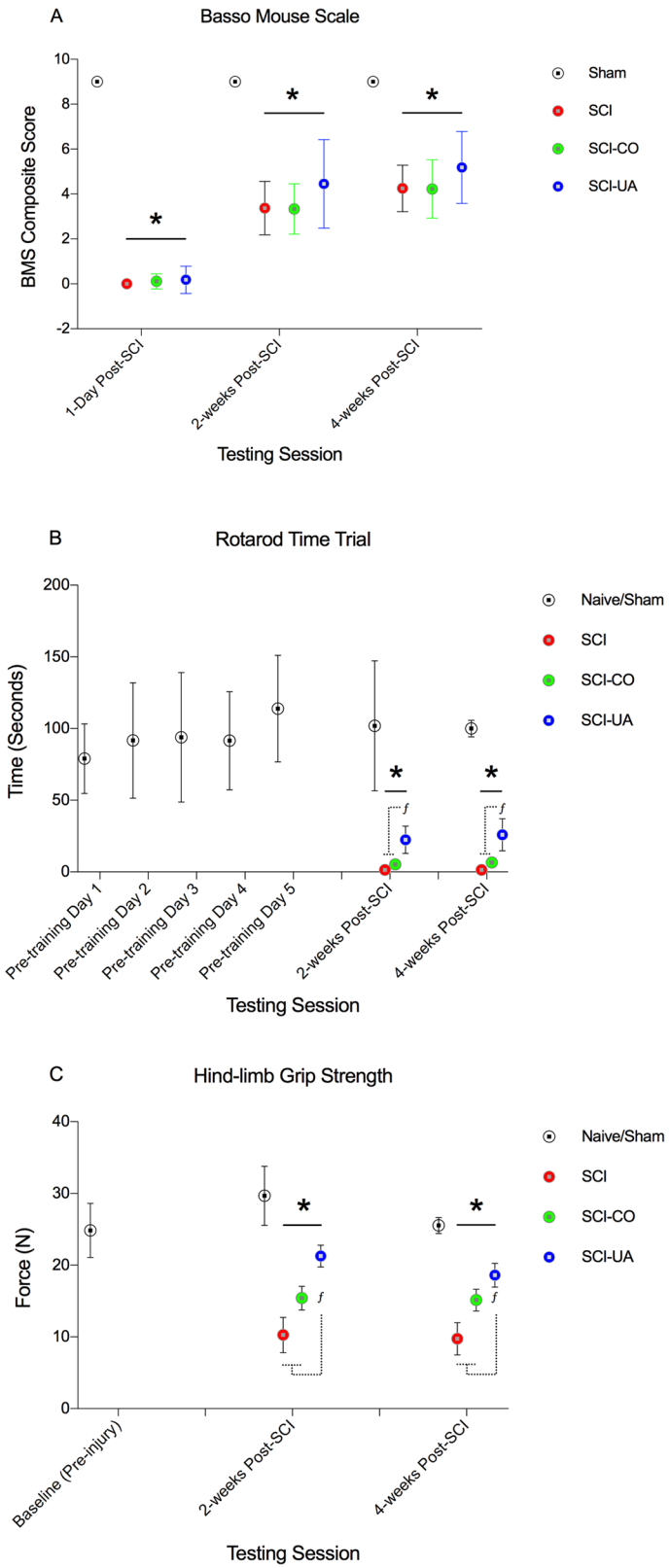

Fig 4. UA treatment improves sub-lesional locomotor outcomes and muscle force production following SCI. A. BMS composite score of locomotor function were significantly decreased in SCI, SCI-CO, and SCI-UA mice at 1-day, 2-, and 4-weeks post-SCI compared to sham controls. At 2- and 4-weeks post-SCI, there was a progressive increase in

all groups, and an observably greater increase in UA treated mice compared to SCI-CO and SCI alone, although not statistically significant. **B.** Rotarod test time was significantly reduced in SCI, SCI-CO, and SCI-UA mice at both 2-, and 4-weeks post-SCI compared to sham controls. UA significantly improved rotarod time at all time-points compared to SCI-CO and SCI alone. **C.** Hind-limb muscle force production (grip strength) was significantly reduced in SCI, SCI-CO, and SCI-UA at 2- and 4-weeks post-SCI compared to sham controls. UA significantly improved grip strength at all time-points compared to SCI-CO and SCI alone. $^{*,f}p < 0.05$.

https://doi.org/10.1371/journal.pone.0203042.g004

rehabilitation strategies like extrinsically stimulated contractions using functional electrical stimulation (FES). Although select studies of long-term FES (6–12 months) have reported on atrophy reversal in acute SCI, [64] and the reversal of fiber type transformation in chronic SCI [65], functional improvements, albeit marginal, have only been observed with long-term FES (up to 16 months) in incomplete SCI. [66, 67] As such, the ability to provide a supplementary countermeasure to these pathological hallmarks on sub-lesional muscle may augment rehabilitation measures using FES and similar intervention paradigms.

SCI results in decentralization of neural connections and loss of contractile activity in the muscle. Although neuromuscular connectivity is maintained, there is impaired trophic support to the muscle, in which reduced neural activity contributes to disuse atrophy and progressive wasting similarly described in various contusion models, [68, 69] spinal isolation [70], denervation [71, 72], and human SCI. [58] The decrease in muscle work diminishes the tissue specific expression of IGF-1 and concomitant autocrine/paracrine mechanisms [73, 74] involving mTOR signaling cascades. [74, 75] Importantly, previous studies indicate downregulation of mTOR and signaling components (including S6K1) in models of chronic SCI. [72, 76] Relevant and opportune literature report that UA enhances IGF-1 and insulin mediated AKT [52] and S6K [53] signaling, two key intermediates in IGF-1/mTOR signaling. This effect of UA on IGF-1/mTOR signaling can independently inhibit atrophy and induce hypertrophy [53], as well as enhance muscle strength. [54] Here, we present data that builds off these previously reported findings and provide further evidence to support the ability of UA treatment to improve activation profiles of PI3K, AKT, mTOR, and S6K. Moreover, we also show that the effect of UA treatment on IGF-1/mTOR signaling translates to measurable physical and functional outcomes like sub-lesional muscle mass and grip strength, respectively, which are significantly greater when compared to untreated injured mice. These results suggest that IGF-1/mTOR signaling has a role in atrophy related pathological processes in SCI, and UA treatment has a protective effect via IGF-1/mTOR signaling that improves muscle related outcomes following SCI. It is important to note that UA may augment divergent pathways involved in hypertrophy. Glycogen synthase kinase 3 beta (GSK3β) is a substrate of AKT and represents an alternate muscle hypertrophy signaling pathway. GSK3β phosphorylation via AKT [77, 78] inactivates its enzymatic activity, which in turn releases 4E-binding protein 1 (4E-BP1) ultimately resulting in translation initiation and protein synthesis. [79] Recent reports also indicate G-protein-coupled receptor-mediated hypertrophy signaling [80] independent of IFG-1/mTOR intermediaries (namely AKT). [81, 82] In particular, Gαi2 pathway has been shown to induce hypertrophy via PKC by negative regulation of GSK3β and activation of S6K1, respectively. This highlights the complexity of hypertrophy signaling cascades in muscle and the need to further examine both individual pathways and signaling integration to clarify the contribution of each pathway under atrophic conditions such as SCI, and better define the effects of treatment strategies such as UA.

Additionally, impaired mTOR signaling results in FOXO1 translocation to the nucleus where it activates catabolic genes involved in proteolysis and cell death. [49, 83–86] This represents a direct link to atrophic pathways involving catabolism and a point of divergence between hypertrophy and atrophy signals. In animal models of SCI and in acute SCI in

humans [72, 76, 87, 88], mRNA expression of FOXO1 is altered, and two muscle-restricted E3 ligases, MAFbx and MuRF-1 –responsible for ubiquitin-mediated protein degradation in skeletal muscle [50]–are also altered, suggesting the ubiquitin-proteasome system (UPS) contributes to skeletal muscle proteolysis in SCI. Here we report the marked increase in FOXO1 mRNA, the *atrogenes* MAFbx, MURF-1 and the proteasomal assembly protein PSMD11 mRNA following SCI, demonstrating the mobilization of UPS-mediated degradation in the muscle. However, as we previously described above regarding hypertrophy signals, the observed increase in these catabolic genes cannot solely be attributed to IGF1/mTOR-mediated signaling, as several pathways are involved in atrophy linked *atrogene* expression and proteolysis in the muscle. For example, pro-inflammatory cytokine (including TNFα and IL-1) signaling activates NF-κB and p38 MAP kinase pathways that induce significant muscle atrophy via MAFbx [89–91] and MURF-1 [92–95] ubiquitin ligases. In addition, there is a growing body of literature confirming the effect of the tumor growth factor β (TGF-β) superfamily peptide, myostatin, in muscle wasting diseases (recently reviewed in [96]). Myostatin is a potent negative regulator of muscle growth [97–102] signaling through serine/threonine type kinase receptors to activate SMAD2/3 transcription factors. Importantly, SMAD target genes include (but are not limited to) ubiquitin-proteasome and autophagy-lysosome systems [103–106], as well as the suppression of myogenic regulatory factors. [107, 108] In addition to SMAD-mediated signaling, myostatin is shown to function in canonical protein synthesis and degradation signaling pathways including mTOR and FOXO1 [109, 110], again demonstrating the complexity and interplay between muscle hypertrophy and atrophy signaling pathways.

Importantly, myopenia occurring after SCI is associated with both substantial loss of sub-lesional muscle mass [13, 16] and fatty infiltration of muscle [16, 111], which together contribute to an obese somatotype [112], reduced whole-body metabolism [113, 114], and increased risk for cardiometabolic disease. [112] Previous rodent studies of SCI contusion and transection have confirmed changes in sub-lesional muscle size and phenotype, [43, 115–117] however, these changes have not been evaluated with respect to accompanying consequences. Beyond its notable trophic effects on skeletal muscle, UA reportedly promotes positive outcomes in models of diabetes and hyperlipidemia [118, 119], making it an attractive treatment strategy for attenuating secondary health complications associated with cardiometabolic disorders in SCI. Although we did not directly address these secondary complications, our data provide evidence that supports future studies to more comprehensively explore consequences of muscle pathology on global metabolism after SCI, and whether UA can mitigate these effects. For example, our current studies using experimental SCI examine phenotypic changes in muscle fiber type, whole body metabolism, serum analysis related to metabolic risk factors, and the relationship between these variables. One limitation here is that we administered UA dissolved in CO, consistent with literature describing UA treatment with atrophic stress. [53, 55] However, CO has a standardized composition which represents a considerable energy and fat source, evident when comparing the body weight curves and soleus weight for SCI, SCI/UA, and SCI/CO treatment groups. The CO alone as an energy substrate may augment body weight and potentially contribute to the lipid infiltration in sub-lesional muscle. Consequently, this obfuscated our examination of outcomes specific to metabolic dysfunction. Future studies will adopt oral or dietary UA administration [120–123] and chronic SCI survival to better address these questions.

Conclusion

Currently there is a lack of effective rehabilitative therapies following SCI. Moreover, a paucity of literature has explored therapies directed at exploiting pathways that contribute to sarcopenia in SCI. Given that UA has shown potential in other paradigms of muscle atrophy, our

findings provide evidence that supports the potential for UA to attenuate muscle-specific pathological consequences of SCI. Further research will help elucidate the potential effect of UA as a viable treatment strategy that may improve muscle health and function following SCI.

Supporting information

S1 Table. Chemiluminescence detection of target proteins in soleus muscle tissue. Shown are normalized relative intensities corresponding to chemiluminescence protein detection from immunoblots targeting the phosphorylated forms of PI3K, AKT, mTOR, and S6K. Groups include sham vs. SCI (1-, 2-, and 4-weeks), and SCI at the same timepoints with UA treatment.
(XLSX)

S2 Table. Quantitative PCR CT Values for catabolic genes in soleus muscle. Shown are CT values for target genes FOXO1, MAFbx, MURF-1, and PSMD11 normalized to Actin ($2^{-\Delta\Delta Ct}$).
(XLSX)

S3 Table. Body mass curves and soleus muscle mass. A complete list of body mass at baseline and daily for 30 days post-SCI. Groups include sham, SCI, SCI with CO, and SCI with UA. Soleus muscle tissue was harvested at time of necropsy at 1-, 2- and 4-weeks post-SCI and mass was recorded. Groups include sham vs. SCI (1-, 2-, and 4-weeks), and SCI at the same timepoints with UA treatment.
(XLSX)

S4 Table. Behavioral and motor function scores. Shown are BMS composite scores for hindlimb locomotor function, rotarod time for motor coordination and balance, and hindlimb grip strength. Values include baseline/pretraining, 1-day, 2- and 4-weeks post-SCI for BMS, and baseline/pretraining, 2- and 4-weeks post-SCI for both rotarod time trial and grip strength.
(XLSX)

Author Contributions

Conceptualization: Gregory E. Bigford.

Data curation: Gregory E. Bigford, Andrew J. Darr, Valerie C. Bracchi-Ricard.

Formal analysis: Gregory E. Bigford, Andrew J. Darr, Valerie C. Bracchi-Ricard.

Funding acquisition: Mark S. Nash, John R. Bethea.

Investigation: Gregory E. Bigford, Andrew J. Darr, Valerie C. Bracchi-Ricard, Han Gao.

Methodology: Gregory E. Bigford, Andrew J. Darr, Valerie C. Bracchi-Ricard, Han Gao.

Supervision: Mark S. Nash, John R. Bethea.

Writing – original draft: Gregory E. Bigford.

Writing – review & editing: Andrew J. Darr, Valerie C. Bracchi-Ricard, Mark S. Nash, John R. Bethea.

References

1. Dearwater SR, LaPorte RE, Robertson RJ, Brenes G, Adams LL, Becker D. Activity in the spinal cord-injured patient: an epidemiologic analysis of metabolic parameters. Med Sci Sports Exerc. 1986; 18 (5):541–4. Epub 1986/10/01. PMID: 3534508.

2. Rodriguez DJ, Benzel EC, Clevenger FW. The metabolic response to spinal cord injury. Spinal Cord. 1997; 35(9):599–604. Epub 1997/09/25. PMID: 9300966.
3. Bauman WA, Spungen AM, Adkins RH, Kemp BJ. Metabolic and endocrine changes in persons aging with spinal cord injury. Assist Technol. 1999; 11(2):88–96. Epub 2000/09/30. https://doi.org/10.1080/10400435.1999.10131993 PMID: 11010069.
4. Bauman WA, Spungen AM. Metabolic changes in persons after spinal cord injury. Phys Med Rehabil Clin N Am. 2000; 11(1):109–40. Epub 2000/02/19. PMID: 10680161.
5. Bauman WA, Spungen AM. Carbohydrate and lipid metabolism in chronic spinal cord injury. J Spinal Cord Med. 2001; 24(4):266–77. Epub 2002/04/12. PMID: 11944785.
6. Kemp BJ. What the rehabilitation professional and the consumer need to know. Phys Med Rehabil Clin N Am. 2005; 16(1):1–18, vii. Epub 2004/11/25. doi: S1047-9651(04)00062-2 [pii] https://doi.org/10.1016/j.pmr.2004.06.009 PMID: 15561542.
7. Groah SaKM. The state of aging and public health for people with spinal cord injury: Lost in transition? Top Spinal Cord Inj Rehabil. 2010; 15:1–10.
8. Grimby G, Broberg C, Krotkiewska I, Krotkiewski M. Muscle fiber composition in patients with traumatic cord lesion. Scand J Rehabil Med. 1976; 8(1):37–42. Epub 1976/01/01. PMID: 132700.
9. Scelsi R, Marchetti C, Poggi P, Lotta S, Lommi G. Muscle fiber type morphology and distribution in paraplegic patients with traumatic cord lesion. Histochemical and ultrastructural aspects of rectus femoris muscle. Acta Neuropathol. 1982; 57(4):243–8. Epub 1982/01/01. PMID: 7136501.
10. Lotta S, Scelsi R, Alfonsi E, Saitta A, Nicolotti D, Epifani P, et al. Morphometric and neurophysiological analysis of skeletal muscle in paraplegic patients with traumatic cord lesion. Paraplegia. 1991; 29(4):247–52. Epub 1991/05/01. https://doi.org/10.1038/sc.1991.35 PMID: 1831255.
11. Round JM, Barr FM, Moffat B, Jones DA. Fibre areas and histochemical fibre types in the quadriceps muscle of paraplegic subjects. J Neurol Sci. 1993; 116(2):207–11. Epub 1993/06/01. PMID: 8336167.
12. Burnham R, Martin T, Stein R, Bell G, MacLean I, Steadward R. Skeletal muscle fibre type transformation following spinal cord injury. Spinal Cord. 1997; 35(2):86–91. Epub 1997/02/01. PMID: 9044514.
13. Castro MJ, Apple DF Jr., Hillegass EA, Dudley GA. Influence of complete spinal cord injury on skeletal muscle cross-sectional area within the first 6 months of injury. Eur J Appl Physiol Occup Physiol. 1999; 80(4):373–8. Epub 1999/09/14. PMID: 10483809.
14. Castro MJ, Apple DF Jr., Staron RS, Campos GE, Dudley GA. Influence of complete spinal cord injury on skeletal muscle within 6 mo of injury. J Appl Physiol (1985). 1999; 86(1):350–8. Epub 1999/01/14. https://doi.org/10.1152/jappl.1999.86.1.350 PMID: 9887150.
15. Modlesky CM, Bickel CS, Slade JM, Meyer RA, Cureton KJ, Dudley GA. Assessment of skeletal muscle mass in men with spinal cord injury using dual-energy X-ray absorptiometry and magnetic resonance imaging. J Appl Physiol (1985). 2004; 96(2):561–5. Epub 2003/10/07. https://doi.org/10.1152/japplphysiol.00207.2003 00207.2003 [pii]. PMID: 14527962.
16. Gorgey AS, Dudley GA. Skeletal muscle atrophy and increased intramuscular fat after incomplete spinal cord injury. Spinal Cord. 2007; 45(4):304–9. Epub 2006/08/31. doi: 3101968 [pii] https://doi.org/10.1038/sj.sc.3101968 PMID: 16940987.
17. Garland DE, Stewart CA, Adkins RH, Hu SS, Rosen C, Liotta FJ, et al. Osteoporosis after spinal cord injury. J Orthop Res. 1992; 10(3):371–8. Epub 1992/05/01. https://doi.org/10.1002/jor.1100100309 PMID: 1569500.
18. Frey-Rindova P, de Bruin ED, Stussi E, Dambacher MA, Dietz V. Bone mineral density in upper and lower extremities during 12 months after spinal cord injury measured by peripheral quantitative computed tomography. Spinal Cord. 2000; 38(1):26–32. Epub 2000/04/13. PMID: 10762194.
19. Zehnder Y, Luthi M, Michel D, Knecht H, Perrelet R, Neto I, et al. Long-term changes in bone metabolism, bone mineral density, quantitative ultrasound parameters, and fracture incidence after spinal cord injury: a cross-sectional observational study in 100 paraplegic men. Osteoporos Int. 2004; 15(3):180–9. Epub 2004/01/15. https://doi.org/10.1007/s00198-003-1529-6 PMID: 14722626.
20. Giangregorio L, McCartney N. Bone loss and muscle atrophy in spinal cord injury: epidemiology, fracture prediction, and rehabilitation strategies. J Spinal Cord Med. 2006; 29(5):489–500. Epub 2007/02/06. PMID: 17274487.
21. Maimoun L, Fattal C, Micallef JP, Peruchon E, Rabischong P. Bone loss in spinal cord-injured patients: from physiopathology to therapy. Spinal Cord. 2006; 44(4):203–10. Epub 2005/09/15. doi: 3101832 [pii] https://doi.org/10.1038/sj.sc.3101832 PMID: 16158075.
22. Qin W, Bauman WA, Cardozo C. Bone and muscle loss after spinal cord injury: organ interactions. Ann N Y Acad Sci. 2010; 1211:66–84. Epub 2010/11/11. https://doi.org/10.1111/j.1749-6632.2010.05806.x PMID: 21062296.

23. Battaglino RA, Lazzari AA, Garshick E, Morse LR. Spinal cord injury-induced osteoporosis: pathogenesis and emerging therapies. Curr Osteoporos Rep. 2012; 10(4):278–85. Epub 2012/09/18. https://doi.org/10.1007/s11914-012-0117-0 PMID: 22983921.

24. Spungen AM, Adkins RH, Stewart CA, Wang J, Pierson RN Jr., Waters RL, et al. Factors influencing body composition in persons with spinal cord injury: a cross-sectional study. J Appl Physiol. 2003; 95 (6):2398–407. Epub 2003/08/12. https://doi.org/10.1152/japplphysiol.00729.2002 00729.2002 [pii]. PMID: 12909613.

25. Gorgey AS, Gater DR. A preliminary report on the effects of the level of spinal cord injury on the association between central adiposity and metabolic profile. PM R. 2011; 3(5):440–6. Epub 2011/05/17. doi: S1934-1482(11)00055-4 [pii] https://doi.org/10.1016/j.pmrj.2011.01.011 PMID: 21570032.

26. Liang H, Chen D, Wang Y, Rimmer JH, Braunschweig CL. Different risk factor patterns for metabolic syndrome in men with spinal cord injury compared with able-bodied men despite similar prevalence rates. Arch Phys Med Rehabil. 2007; 88(9):1198–204. Epub 2007/09/11. doi: S0003-9993(07)00384-X [pii] https://doi.org/10.1016/j.apmr.2007.05.023 PMID: 17826468.

27. Groah SL, Nash MS, Ljungberg IH, Libin A, Hamm LF, Ward E, et al. Nutrient intake and body habitus after spinal cord injury: an analysis by sex and level of injury. J Spinal Cord Med. 2009; 32(1):25–33. Epub 2009/03/07. PMID: 19264046.

28. Groah SL, Nash MS, Ward EA, Libin A, Mendez AJ, Burns P, et al. Cardiometabolic risk in community-dwelling persons with chronic spinal cord injury. J Cardiopulm Rehabil Prev. 2011; 31(2):73–80. Epub 2010/11/04. https://doi.org/10.1097/HCR.0b013e3181f68aba PMID: 21045711.

29. Brenes G, Dearwater S, Shapera R, LaPorte RE, Collins E. High density lipoprotein cholesterol concentrations in physically active and sedentary spinal cord injured patients. Arch Phys Med Rehabil. 1986; 67(7):445–50. Epub 1986/07/01. doi: 0003-9993(86)90256-X [pii]. PMID: 3729689.

30. Bauman WA, Spungen AM, Zhong YG, Rothstein JL, Petry C, Gordon SK. Depressed serum high density lipoprotein cholesterol levels in veterans with spinal cord injury. Paraplegia. 1992; 30(10):697–703. Epub 1992/10/01. https://doi.org/10.1038/sc.1992.136 PMID: 1448297.

31. Zlotolow SP, Levy E, Bauman WA. The serum lipoprotein profile in veterans with paraplegia: the relationship to nutritional factors and body mass index. J Am Paraplegia Soc. 1992; 15(3):158–62. Epub 1992/07/01. PMID: 1500941.

32. Karlsson AK, Attvall S, Jansson PA, Sullivan L, Lonnroth P. Influence of the sympathetic nervous system on insulin sensitivity and adipose tissue metabolism: a study in spinal cord-injured subjects. Metabolism. 1995; 44(1):52–8. Epub 1995/01/01. PMID: 7854166.

33. Maki KC, Briones ER, Langbein WE, Inman-Felton A, Nemchausky B, Welch M, et al. Associations between serum lipids and indicators of adiposity in men with spinal cord injury. Paraplegia. 1995; 33 (2):102–9. Epub 1995/02/01. https://doi.org/10.1038/sc.1995.24 PMID: 7753565.

34. McGlinchey-Berroth R, Morrow L, Ahlquist M, Sarkarati M, Minaker KL. Late-life spinal cord injury and aging with a long term injury: characteristics of two emerging populations. J Spinal Cord Med. 1995; 18 (3):183–93. Epub 1995/07/01. PMID: 7552423.

35. Bauman WA, Kahn NN, Grimm DR, Spungen AM. Risk factors for atherogenesis and cardiovascular autonomic function in persons with spinal cord injury. Spinal Cord. 1999; 37(9):601–16. Epub 1999/09/22. PMID: 10490851.

36. Wahman K, Nash MS, Lewis JE, Seiger A, Levi R. Cardiovascular disease risk and the need for prevention after paraplegia determined by conventional multifactorial risk models: the Stockholm spinal cord injury study. J Rehabil Med. 2011; 43(3):237–42. Epub 2011/02/10. https://doi.org/10.2340/16501977-0658 PMID: 21305240.

37. Chen Y, Henson S, Jackson AB, Richards JS. Obesity intervention in persons with spinal cord injury. Spinal Cord. 2006; 44(2):82–91. Epub 2005/08/17. doi: 3101818 [pii] https://doi.org/10.1038/sj.sc.3101818 PMID: 16103891.

38. Garshick E, Kelley A, Cohen SA, Garrison A, Tun CG, Gagnon D, et al. A prospective assessment of mortality in chronic spinal cord injury. Spinal Cord. 2005; 43(7):408–16. Epub 2005/02/16. doi: 3101729 [pii] https://doi.org/10.1038/sj.sc.3101729 PMID: 15711609.

39. Myers J, Lee M, Kiratli J. Cardiovascular disease in spinal cord injury: an overview of prevalence, risk, evaluation, and management. Am J Phys Med Rehabil. 2007; 86(2):142–52. Epub 2007/01/26. https://doi.org/10.1097/PHM.0b013e31802f0247 00002060-200702000-00009 [pii]. PMID: 17251696.

40. Shields RK. Fatigability, relaxation properties, and electromyographic responses of the human paralyzed soleus muscle. J Neurophysiol. 1995; 73(6):2195–206. Epub 1995/06/01. https://doi.org/10.1152/jn.1995.73.6.2195 PMID: 7666132.

41. Shields RK, Law LF, Reiling B, Sass K, Wilwert J. Effects of electrically induced fatigue on the twitch and tetanus of paralyzed soleus muscle in humans. J Appl Physiol (1985). 1997; 82(5):1499–507. Epub 1997/05/01. https://doi.org/10.1152/jappl.1997.82.5.1499 PMID: 9134899.

42. Gerrits HL, De Haan A, Hopman MT, van Der Woude LH, Jones DA, Sargeant AJ. Contractile properties of the quadriceps muscle in individuals with spinal cord injury. Muscle Nerve. 1999; 22(9):1249–56. Epub 1999/08/24. https://doi.org/10.1002/(SICI)1097-4598(199909)22:9<1249::AID-MUS13>3.0.CO;2-N [pii]. PMID: 10454722.

43. Talmadge RJ, Roy RR, Caiozzo VJ, Edgerton VR. Mechanical properties of rat soleus after long-term spinal cord transection. J Appl Physiol (1985). 2002; 93(4):1487–97. Epub 2002/09/18. https://doi.org/10.1152/japplphysiol.00053.2002 PMID: 12235051.

44. Grange RW, Gainer TG, Marschner KM, Talmadge RJ, Stull JT. Fast-twitch skeletal muscles of dystrophic mouse pups are resistant to injury from acute mechanical stress. Am J Physiol Cell Physiol. 2002; 283(4):C1090–101. Epub 2002/09/13. https://doi.org/10.1152/ajpcell.00450.2001 PMID: 12225973.

45. Tsitouras PD, Zhong YG, Spungen AM, Bauman WA. Serum testosterone and growth hormone/insulin-like growth factor-I in adults with spinal cord injury. Horm Metab Res. 1995; 27(6):287–92. Epub 1995/06/01. https://doi.org/10.1055/s-2007-979961 PMID: 7557841.

46. Kostovski E, Iversen PO, Birkeland K, Torjesen PA, Hjeltnes N. Decreased levels of testosterone and gonadotrophins in men with long-standing tetraplegia. Spinal Cord. 2008; 46(8):559–64. Epub 2008/03/05. https://doi.org/10.1038/sc.2008.3 sc20083 [pii]. PMID: 18317482.

47. Laplante M, Sabatini DM. mTOR signaling in growth control and disease. Cell. 2012; 149(2):274–93. Epub 2012/04/17. https://doi.org/10.1016/j.cell.2012.03.017 S0092-8674(12)00351-0 [pii]. PMID: 22500797.

48. Koopman R, Ly CH, Ryall JG. A metabolic link to skeletal muscle wasting and regeneration. Front Physiol. 2014; 5:32. Epub 2014/02/26. https://doi.org/10.3389/fphys.2014.00032 PMID: 24567722.

49. Leger B, Cartoni R, Praz M, Lamon S, Deriaz O, Crettenand A, et al. Akt signalling through GSK-3beta, mTOR and Foxo1 is involved in human skeletal muscle hypertrophy and atrophy. J Physiol. 2006; 576(Pt 3):923–33. Epub 2006/08/19. doi: jphysiol.2006.116715 [pii] https://doi.org/10.1113/jphysiol.2006.116715 PMID: 16916907.

50. Bodine SC, Latres E, Baumhueter S, Lai VK, Nunez L, Clarke BA, et al. Identification of ubiquitin ligases required for skeletal muscle atrophy. Science. 2001; 294(5547):1704–8. Epub 2001/10/27. https://doi.org/10.1126/science.1065874 1065874 [pii]. PMID: 11679633.

51. Novotny L, Vachalkova A, Biggs D. Ursolic acid: an anti-tumorigenic and chemopreventive activity. Minireview. Neoplasma. 2001; 48(4):241–6. Epub 2001/11/20. PMID: 11712672.

52. Jung SH, Ha YJ, Shim EK, Choi SY, Jin JL, Yun-Choi HS, et al. Insulin-mimetic and insulin-sensitizing activities of a pentacyclic triterpenoid insulin receptor activator. Biochem J. 2007; 403(2):243–50. Epub 2007/01/05. https://doi.org/10.1042/BJ20061123 PMID: 17201692; PubMed Central PMCID: PMCPMC1874232.

53. Kunkel SD, Suneja M, Ebert SM, Bongers KS, Fox DK, Malmberg SE, et al. mRNA expression signatures of human skeletal muscle atrophy identify a natural compound that increases muscle mass. Cell Metab. 2011; 13(6):627–38. Epub 2011/06/07. https://doi.org/10.1016/j.cmet.2011.03.020 S1550-4131(11)00177-X [pii]. PMID: 21641545.

54. Bang HS, Seo DY, Chung YM, Oh KM, Park JJ, Arturo F, et al. Ursolic Acid-induced elevation of serum irisin augments muscle strength during resistance training in men. Korean J Physiol Pharmacol. 2014; 18(5):441–6. Epub 2014/10/30. https://doi.org/10.4196/kjpp.2014.18.5.441 PMID: 25352765.

55. Ogasawara R, Sato K, Higashida K, Nakazato K, Fujita S. Ursolic acid stimulates mTORC1 signaling after resistance exercise in rat skeletal muscle. Am J Physiol Endocrinol Metab. 2013; 305(6):E760–5. Epub 2013/08/01. https://doi.org/10.1152/ajpendo.00302.2013 PMID: 23900420.

56. Basso DM, Fisher LC, Anderson AJ, Jakeman LB, McTigue DM, Popovich PG. Basso Mouse Scale for locomotion detects differences in recovery after spinal cord injury in five common mouse strains. J Neurotrauma. 2006; 23(5):635–59. Epub 2006/05/13. https://doi.org/10.1089/neu.2006.23.635 PMID: 16689667.

57. Nishi RA, Liu H, Chu Y, Hamamura M, Su MY, Nalcioglu O, et al. Behavioral, histological, and ex vivo magnetic resonance imaging assessment of graded contusion spinal cord injury in mice. J Neurotrauma. 2007; 24(4):674–89. https://doi.org/10.1089/neu.2006.0204 PMID: 17439350.

58. Thomas CK, Zaidner EY, Calancie B, Broton JG, Bigland-Ritchie BR. Muscle weakness, paralysis, and atrophy after human cervical spinal cord injury. Exp Neurol. 1997; 148(2):414–23. Epub 1998/01/24. https://doi.org/10.1006/exnr.1997.6690 PMID: 9417821.

59. Levy M, Mizrahi J, Susak Z. Recruitment, force and fatigue characteristics of quadriceps muscles of paraplegics isometrically activated by surface functional electrical stimulation. J Biomed Eng. 1990; 12(2):150–6. Epub 1990/03/01. PMID: 2319765.

60. Rabischong E, Ohanna F. Effects of functional electrical stimulation (FES) on evoked muscular output in paraplegic quadriceps muscle. Paraplegia. 1992; 30(7):467–73. Epub 1992/07/01. https://doi.org/10.1038/sc.1992.100 PMID: 1508560.

61. Rochester L, Chandler CS, Johnson MA, Sutton RA, Miller S. Influence of electrical stimulation of the tibialis anterior muscle in paraplegic subjects. 1. Contractile properties. Paraplegia. 1995; 33(8):437–49. Epub 1995/08/01. https://doi.org/10.1038/sc.1995.102 PMID: 7478737.

62. Gordon T, Mao J. Muscle atrophy and procedures for training after spinal cord injury. Phys Ther. 1994; 74(1):50–60. Epub 1994/01/01. PMID: 8265728.

63. Dudley-Javoroski S, Shields RK. Muscle and bone plasticity after spinal cord injury: review of adaptations to disuse and to electrical muscle stimulation. J Rehabil Res Dev. 2008; 45(2):283–96. Epub 2008/06/21. PMID: 18566946; PubMed Central PMCID: PMCPMC2744487.

64. Baldi JC, Jackson RD, Moraille R, Mysiw WJ. Muscle atrophy is prevented in patients with acute spinal cord injury using functional electrical stimulation. Spinal Cord. 1998; 36(7):463–9. Epub 1998/07/22. PMID: 9670381.

65. Andersen JL, Mohr T, Biering-Sorensen F, Galbo H, Kjaer M. Myosin heavy chain isoform transformation in single fibres from m. vastus lateralis in spinal cord injured individuals: effects of long-term functional electrical stimulation (FES). Pflugers Arch. 1996; 431(4):513–8. Epub 1996/02/01. PMID: 8596693.

66. Donaldson N, Perkins TA, Fitzwater R, Wood DE, Middleton F. FES cycling may promote recovery of leg function after incomplete spinal cord injury. Spinal Cord. 2000; 38(11):680–2. Epub 2000/12/15. PMID: 11114775.

67. Granat MH, Ferguson AC, Andrews BJ, Delargy M. The role of functional electrical stimulation in the rehabilitation of patients with incomplete spinal cord injury—observed benefits during gait studies. Paraplegia. 1993; 31(4):207–15. Epub 1993/04/01. https://doi.org/10.1038/sc.1993.39 PMID: 8493035.

68. Lin CY, Androjna C, Rozic R, Nguyen BT, Parsons B, Midura RJ, et al. Differential adaptations of the musculoskeletal system following spinal cord contusion and transection in rats. J Neurotrauma. 2018. Epub 2018/02/07. https://doi.org/10.1089/neu.2017.5444 PMID: 29402167.

69. Ohnishi Y, Iwatsuki K, Shinzawa K, Nakai Y, Ishihara M, Yoshimine T. Disuse muscle atrophy exacerbates motor neuronal degeneration caudal to the site of spinal cord injury. Neuroreport. 2012; 23 (3):157–61. Epub 2011/12/21. https://doi.org/10.1097/WNR.0b013e32834f4048 PMID: 22182976.

70. Roy RR, Kim JA, Grossman EJ, Bekmezian A, Talmadge RJ, Zhong H, et al. Persistence of myosin heavy chain-based fiber types in innervated but silenced rat fast muscle. Muscle Nerve. 2000; 23 (5):735–47. Epub 2000/05/08. PMID: 10797397.

71. Muller FL, Song W, Jang YC, Liu Y, Sabia M, Richardson A, et al. Denervation-induced skeletal muscle atrophy is associated with increased mitochondrial ROS production. Am J Physiol Regul Integr Comp Physiol. 2007; 293(3):R1159–68. Epub 2007/06/23. https://doi.org/10.1152/ajpregu.00767.2006 PMID: 17584954.

72. Sacheck JM, Hyatt JP, Raffaello A, Jagoe RT, Roy RR, Edgerton VR, et al. Rapid disuse and denervation atrophy involve transcriptional changes similar to those of muscle wasting during systemic diseases. FASEB J. 2007; 21(1):140–55. Epub 2006/11/23. https://doi.org/10.1096/fj.06-6604com PMID: 17116744.

73. DeVol DL, Rotwein P, Sadow JL, Novakofski J, Bechtel PJ. Activation of insulin-like growth factor gene expression during work-induced skeletal muscle growth. Am J Physiol. 1990; 259(1 Pt 1):E89–95. Epub 1990/07/01. https://doi.org/10.1152/ajpendo.1990.259.1.E89 PMID: 2372054.

74. Glass DJ. Signalling pathways that mediate skeletal muscle hypertrophy and atrophy. Nat Cell Biol. 2003; 5(2):87–90. Epub 2003/02/04. https://doi.org/10.1038/ncb0203-87 PMID: 12563267.

75. Zhang H, Stallock JP, Ng JC, Reinhard C, Neufeld TP. Regulation of cellular growth by the Drosophila target of rapamycin dTOR. Genes Dev. 2000; 14(21):2712–24. Epub 2000/11/09. PMID: 11069888; PubMed Central PMCID: PMCPMC317034.

76. Zeman RJ, Zhao J, Zhang Y, Zhao W, Wen X, Wu Y, et al. Differential skeletal muscle gene expression after upper or lower motor neuron transection. Pflugers Arch. 2009; 458(3):525–35. Epub 2009/02/14. https://doi.org/10.1007/s00424-009-0643-5 PMID: 19214561.

77. Hajduch E, Alessi DR, Hemmings BA, Hundal HS. Constitutive activation of protein kinase B alpha by membrane targeting promotes glucose and system A amino acid transport, protein synthesis, and inactivation of glycogen synthase kinase 3 in L6 muscle cells. Diabetes. 1998; 47(7):1006–13. Epub 1998/07/02. PMID: 9648821.

78. van Weeren PC, de Bruyn KM, de Vries-Smits AM, van Lint J, Burgering BM. Essential role for protein kinase B (PKB) in insulin-induced glycogen synthase kinase 3 inactivation. Characterization of dominant-negative mutant of PKB. J Biol Chem. 1998; 273(21):13150–6. Epub 1998/05/28. PMID: 9582355.

79. Rhoads RE. Signal transduction pathways that regulate eukaryotic protein synthesis. J Biol Chem. 1999; 274(43):30337–40. Epub 1999/10/16. PMID: 10521405.

80. Minetti GC, Feige JN, Rosenstiel A, Bombard F, Meier V, Werner A, et al. Galphai2 signaling promotes skeletal muscle hypertrophy, myoblast differentiation, and muscle regeneration. Sci Signal. 2011; 4 (201):ra80. Epub 2011/12/01. https://doi.org/10.1126/scisignal.2002038 PMID: 22126963.

81. Egerman MA, Glass DJ. Signaling pathways controlling skeletal muscle mass. Crit Rev Biochem Mol Biol. 2014; 49(1):59–68. Epub 2013/11/19. https://doi.org/10.3109/10409238.2013.857291 PMID: 24237131; PubMed Central PMCID: PMCPMC3913083.

82. Jean-Baptiste G, Yang Z, Khoury C, Gaudio S, Greenwood MT. Peptide and non-peptide G-protein coupled receptors (GPCRs) in skeletal muscle. Peptides. 2005; 26(8):1528–36. Epub 2005/07/27. https://doi.org/10.1016/j.peptides.2005.03.011 PMID: 16042993.

83. Bodine SC, Stitt TN, Gonzalez M, Kline WO, Stover GL, Bauerlein R, et al. Akt/mTOR pathway is a crucial regulator of skeletal muscle hypertrophy and can prevent muscle atrophy in vivo. Nat Cell Biol. 2001; 3(11):1014–9. Epub 2001/11/21. https://doi.org/10.1038/ncb1101-1014 ncb1101-1014 [pii]. PMID: 11715023.

84. Sandri M, Sandri C, Gilbert A, Skurk C, Calabria E, Picard A, et al. Foxo transcription factors induce the atrophy-related ubiquitin ligase atrogin-1 and cause skeletal muscle atrophy. Cell. 2004; 117 (3):399–412. Epub 2004/04/28. doi: S0092867404004003 [pii]. PMID: 15109499.

85. Stitt TN, Drujan D, Clarke BA, Panaro F, Timofeyva Y, Kline WO, et al. The IGF-1/PI3K/Akt pathway prevents expression of muscle atrophy-induced ubiquitin ligases by inhibiting FOXO transcription factors. Mol Cell. 2004; 14(3):395–403. Epub 2004/05/06. doi: S1097276504002114 [pii]. PMID: 15125842.

86. Urso ML. Disuse atrophy of human skeletal muscle: cell signaling and potential interventions. Med Sci Sports Exerc. 2009; 41(10):1860–8. Epub 2009/09/04. https://doi.org/10.1249/MSS.0b013e3181a6458a PMID: 19727028.

87. Urso ML, Chen YW, Scrimgeour AG, Lee PC, Lee KF, Clarkson PM. Alterations in mRNA expression and protein products following spinal cord injury in humans. J Physiol. 2007; 579(Pt 3):877–92. Epub 2007/01/16. doi: jphysiol.2006.118042 [pii] https://doi.org/10.1113/jphysiol.2006.118042 PMID: 17218363.

88. Leger B, Senese R, Al-Khodairy AW, Deriaz O, Gobelet C, Giacobino JP, et al. Atrogin-1, MuRF1, and FoXO, as well as phosphorylated GSK-3beta and 4E-BP1 are reduced in skeletal muscle of chronic spinal cord-injured patients. Muscle Nerve. 2009; 40(1):69–78. Epub 2009/06/18. https://doi.org/10.1002/mus.21293 PMID: 19533653.

89. Csibi A, Leibovitch MP, Cornille K, Tintignac LA, Leibovitch SA. MAFbx/Atrogin-1 controls the activity of the initiation factor eIF3-f in skeletal muscle atrophy by targeting multiple C-terminal lysines. J Biol Chem. 2009; 284(7):4413–21. Epub 2008/12/17. https://doi.org/10.1074/jbc.M807641200 PMID: 19073596.

90. Lagirand-Cantaloube J, Offner N, Csibi A, Leibovitch MP, Batonnet-Pichon S, Tintignac LA, et al. The initiation factor eIF3-f is a major target for atrogin1/MAFbx function in skeletal muscle atrophy. EMBO J. 2008; 27(8):1266–76. Epub 2008/03/21. https://doi.org/10.1038/emboj.2008.52 PMID: 18354498; PubMed Central PMCID: PMCPMC2367397.

91. Sanchez AM, Csibi A, Raibon A, Docquier A, Lagirand-Cantaloube J, Leibovitch MP, et al. eIF3f: a central regulator of the antagonism atrophy/hypertrophy in skeletal muscle. Int J Biochem Cell Biol. 2013; 45(10):2158–62. Epub 2013/06/19. https://doi.org/10.1016/j.biocel.2013.06.001 PMID: 23769948.

92. Cai D, Frantz JD, Tawa NE Jr., Melendez PA, Oh BC, Lidov HG, et al. IKKbeta/NF-kappaB activation causes severe muscle wasting in mice. Cell. 2004; 119(2):285–98. Epub 2004/10/14. https://doi.org/10.1016/j.cell.2004.09.027 PMID: 15479644.

93. Glass DJ. Skeletal muscle hypertrophy and atrophy signaling pathways. Int J Biochem Cell Biol. 2005; 37(10):1974–84. Epub 2005/08/10. https://doi.org/10.1016/j.biocel.2005.04.018 PMID: 16087388.

94. Clarke BA, Drujan D, Willis MS, Murphy LO, Corpina RA, Burova E, et al. The E3 Ligase MuRF1 degrades myosin heavy chain protein in dexamethasone-treated skeletal muscle. Cell Metab. 2007; 6 (5):376–85. Epub 2007/11/07. https://doi.org/10.1016/j.cmet.2007.09.009 PMID: 17983583.

95. Cohen S, Brault JJ, Gygi SP, Glass DJ, Valenzuela DM, Gartner C, et al. During muscle atrophy, thick, but not thin, filament components are degraded by MuRF1-dependent ubiquitylation. J Cell Biol. 2009; 185(6):1083–95. Epub 2009/06/10. https://doi.org/10.1083/jcb.200901052 PMID: 19506036; PubMed Central PMCID: PMCPMC2711608.

96. Elkina Y, von Haehling S, Anker SD, Springer J. The role of myostatin in muscle wasting: an overview. J Cachexia Sarcopenia Muscle. 2011; 2(3):143–51. Epub 2011/10/04. https://doi.org/10.1007/s13539-011-0035-5 PMID: 21966641; PubMed Central PMCID: PMCPMC3177043.

97. Lee SJ, McPherron AC. Myostatin and the control of skeletal muscle mass. Curr Opin Genet Dev. 1999; 9(5):604–7. Epub 1999/10/06. PMID: 10508689.

98. Lee SJ, McPherron AC. Regulation of myostatin activity and muscle growth. Proc Natl Acad Sci U S A. 2001; 98(16):9306–11. Epub 2001/07/19. https://doi.org/10.1073/pnas.151270098 PMID: 11459935; PubMed Central PMCID: PMCPMC55416.

99. McPherron AC, Lee SJ. Double muscling in cattle due to mutations in the myostatin gene. Proc Natl Acad Sci U S A. 1997; 94(23):12457–61. Epub 1997/11/14. PMID: 9356471; PubMed Central PMCID: PMCPMC24998.

100. McPherron AC, Lee SJ. Suppression of body fat accumulation in myostatin-deficient mice. J Clin Invest. 2002; 109(5):595–601. Epub 2002/03/06. https://doi.org/10.1172/JCI13562 PMID: 11877467; PubMed Central PMCID: PMCPMC150888.

101. McPherron AC, Lawler AM, Lee SJ. Regulation of skeletal muscle mass in mice by a new TGF-beta superfamily member. Nature. 1997; 387(6628):83–90. Epub 1997/05/01. https://doi.org/10.1038/387083a0 PMID: 9139826.

102. McPherron AC, Lawler AM, Lee SJ. Regulation of anterior/posterior patterning of the axial skeleton by growth/differentiation factor 11. Nat Genet. 1999; 22(3):260–4. Epub 1999/07/03. https://doi.org/10.1038/10320 PMID: 10391213.

103. Garikipati DK, Rodgers BD. Myostatin stimulates myosatellite cell differentiation in a novel model system: evidence for gene subfunctionalization. Am J Physiol Regul Integr Comp Physiol. 2012; 302(9): R1059–66. https://doi.org/10.1152/ajpregu.00523.2011 PMID: 22262307.

104. Lee JY, Hopkinson NS, Kemp PR. Myostatin induces autophagy in skeletal muscle in vitro. Biochem Biophys Res Commun. 2011; 415(4):632–6. https://doi.org/10.1016/j.bbrc.2011.10.124 PMID: 22079631.

105. Rodriguez J, Vernus B, Chelh I, Cassar-Malek I, Gabillard JC, Hadj Sassi A, et al. Myostatin and the skeletal muscle atrophy and hypertrophy signaling pathways. Cell Mol Life Sci. 2014; 71(22):4361–71. Epub 2014/08/01. https://doi.org/10.1007/s00018-014-1689-x PMID: 25080109.

106. Seiliez I, Taty Taty GC, Bugeon J, Dias K, Sabin N, Gabillard JC. Myostatin induces atrophy of trout myotubes through inhibiting the TORC1 signaling and promoting Ubiquitin-Proteasome and Autophagy-Lysosome degradative pathways. Gen Comp Endocrinol. 2013; 186:9–15. https://doi.org/10.1016/j.ygcen.2013.02.008 PMID: 23458288.

107. Huang Z, Chen X, Chen D. Myostatin: a novel insight into its role in metabolism, signal pathways, and expression regulation. Cell Signal. 2011; 23(9):1441–6. https://doi.org/10.1016/j.cellsig.2011.05.003 PMID: 21609762.

108. Shi Y, Massague J. Mechanisms of TGF-beta signaling from cell membrane to the nucleus. Cell. 2003; 113(6):685–700. PMID: 12809600.

109. Chelh I, Meunier B, Picard B, Reecy MJ, Chevalier C, Hocquette JF, et al. Molecular profiles of Quadriceps muscle in myostatin-null mice reveal PI3K and apoptotic pathways as myostatin targets. BMC Genomics. 2009; 10:196. https://doi.org/10.1186/1471-2164-10-196 PMID: 19397818; PubMed Central PMCID: PMCPMC2684550.

110. Chelh I, Picard B, Hocquette JF, Cassar-Malek I. Myostatin inactivation induces a similar muscle molecular signature in double-muscled cattle as in mice. Animal. 2011; 5(2):278–86. https://doi.org/10.1017/S1751731110001862 PMID: 22440772.

111. Moore CD, Craven BC, Thabane L, Laing AC, Frank-Wilson AW, Kontulainen SA, et al. Lower-extremity muscle atrophy and fat infiltration after chronic spinal cord injury. J Musculoskelet Neuronal Interact. 2015; 15(1):32–41. Epub 2015/03/03. PMID: 25730650; PubMed Central PMCID: PMCPMC5092153.

112. Nash MS, Tractenberg RE, Mendez AJ, David M, Ljungberg IH, Tinsley EA, et al. Cardiometabolic Syndrome in People With Spinal Cord Injury/Disease: Guideline-Derived and Nonguideline Risk Components in a Pooled Sample. Arch Phys Med Rehabil. 2016; 97(10):1696–705. Epub 2016/07/29. https://doi.org/10.1016/j.apmr.2016.07.002 PMID: 27465752.

113. Nash MS. Exercise as a health-promoting activity following spinal cord injury. J Neurol Phys Ther. 2005; 29(2):87–103, 6. Epub 2006/01/03. PMID: 16386165.

114. Nash MS, Bilsker MS, Kearney HM, Ramirez JN, Applegate B, Green BA. Effects of electrically-stimulated exercise and passive motion on echocardiographically-derived wall motion and cardiodynamic function in tetraplegic persons. Paraplegia. 1995; 33(2):80–9. Epub 1995/02/01. https://doi.org/10.1038/sc.1995.20 PMID: 7753573.

115. Dupont-Versteegden EE, Murphy RJ, Houle JD, Gurley CM, Peterson CA. Mechanisms leading to restoration of muscle size with exercise and transplantation after spinal cord injury. Am J Physiol Cell Physiol. 2000; 279(6):C1677–84. Epub 2000/11/18. https://doi.org/10.1152/ajpcell.2000.279.6.C1677 PMID: 11078681.

116. Lieber RL. Skeletal muscle adaptability. II: Muscle properties following spinal-cord injury. Dev Med Child Neurol. 1986; 28(4):533–42. Epub 1986/08/01. PMID: 3530860.

117. Wei ZJ, Zhou XH, Fan BY, Lin W, Ren YM, Feng SQ. Proteomic and bioinformatic analyses of spinal cord injuryinduced skeletal muscle atrophy in rats. Mol Med Rep. 2016; 14(1):165–74. Epub 2016/05/14. https://doi.org/10.3892/mmr.2016.5272 PMID: 27177391; PubMed Central PMCID: PMCPMC4918545.

118. Liu J. Oleanolic acid and ursolic acid: research perspectives. J Ethnopharmacol. 2005; 100(1–2):92–4. Epub 2005/07/05. https://doi.org/10.1016/j.jep.2005.05.024 PMID: 15994040.

119. Wang ZH, Hsu CC, Huang CN, Yin MC. Anti-glycative effects of oleanolic acid and ursolic acid in kidney of diabetic mice. Eur J Pharmacol. 2010; 628(1–3):255–60. Epub 2009/11/18. https://doi.org/10.1016/j.ejphar.2009.11.019 PMID: 19917277.

120. Chu X, He X, Shi Z, Li C, Guo F, Li S, et al. Ursolic acid increases energy expenditure through enhancing free fatty acid uptake and beta-oxidation via an UCP3/AMPK-dependent pathway in skeletal muscle. Mol Nutr Food Res. 2015; 59(8):1491–503. Epub 2015/05/07. https://doi.org/10.1002/mnfr.201400670 PMID: 25944715.

121. Jia Y, Kim S, Kim J, Kim B, Wu C, Lee JH, et al. Ursolic acid improves lipid and glucose metabolism in high-fat-fed C57BL/6J mice by activating peroxisome proliferator-activated receptor alpha and hepatic autophagy. Mol Nutr Food Res. 2015; 59(2):344–54. https://doi.org/10.1002/mnfr.201400399 PMID: 25418615.

122. Kunkel SD, Elmore CJ, Bongers KS, Ebert SM, Fox DK, Dyle MC, et al. Ursolic acid increases skeletal muscle and brown fat and decreases diet-induced obesity, glucose intolerance and fatty liver disease. PLoS One. 2012; 7(6):e39332. Epub 2012/06/30. https://doi.org/10.1371/journal.pone.0039332 PMID: 22745735; PubMed Central PMCID: PMCPMC3379974.

123. Yang Y, Li C, Xiang X, Dai Z, Chang J, Zhang M, et al. Ursolic acid prevents endoplasmic reticulum stress-mediated apoptosis induced by heat stress in mouse cardiac myocytes. J Mol Cell Cardiol. 2014; 67:103–11. Epub 2014/01/07. https://doi.org/10.1016/j.yjmcc.2013.12.018 PMID: 24389342.